Available online at www.sciencedirect.com

ScienceDirect

journal homepage: www.jfda-online.com

Original Article

A highly sensitive ultra-high performance liquid chromatography/tandem mass spectrometry method with in-source fragmentation for rapid quantification of raspberry ketone

Bo Yuan [a,b], *Danyue Zhao* [a], *Ruoyuan Du* [b], *Dushyant Kshatriya* [c], *Nicholas T. Bello* [c], *James E. Simon* [a], *Qingli Wu* [a,b,*]

[a] *New Use Agriculture and Natural Plant Products Program, Department of Plant Biology, Rutgers University, 59 Dudley Road, New Brunswick, NJ 08901, USA*

[b] *Department of Food Science, Rutgers University, 65 Dudley Road, New Brunswick, NJ 08901, USA*

[c] *Department of Animal Sciences and Nutritional Sciences Graduate Program, Rutgers University, 84 Lipman Drive, New Brunswick, NJ 08901, USA*

ARTICLE INFO

Article history:
Received 8 June 2018
Received in revised form
25 July 2018
Accepted 30 July 2018
Available online 14 August 2018

Keywords:
Raspberry
Raspberry ketone
LC-MS/MS
In-source fragmentation
Factorial design

ABSTRACT

Raspberry ketone (RK) is the characteristic aromatic compound in raspberry (*Rubus idaeus* L.) with wide applications as food additive and anti-obesity agent. However, quantification of RK has presented difficulties in MS detection and reliable LC-MS method for RK analysis in literature is in limit to date. In order to facilitate quality control of raspberry derived products and RK metabolomics study, this study aimed to develop a validated and sensitive UHPLC-MS/MS method. Strong in-source fragmentation was noted and the fragmental ion of 107 *m/z* produced was selected as the precursor ion for MRM detection, and as such the electrospray ionization performance was optimized by fractional factorial design to accommodate such ion-source dissociation behavior as well as its moderate volatility. A pathway involving the formation of quinone-like structure with strong conjugation was proposed to explain the intense in-source fragmentation. The MRM transition was optimized with product ion of 77 *m/z* selected as the quantifier ion. The method featured low limit of quantification of ~2 ng/mL and allowed for rapid detection of RK in fresh raspberries following direct sample preparation. RK contents were found to be higher from locally grown and harvested farm sources compared to commercial products shipped into the state, and higher in those at late-stage compared with early-stage maturity. No correlations in RK content between organic and non-organic labels were noted.

* *Corresponding author*. Department of Plant Biology, Rutgers University, 59 Dudley Road, New Brunswick, NJ 08901, USA.
E-mail address: qlwu@sebs.rutgers.edu (Q. Wu).

https://doi.org/10.1016/j.jfda.2018.07.005

1. Introduction

Red raspberry (*Rubus idaeus* L.) has been a commonly consumed berry fruit for hundreds of years and remains a highly popular fruit. The appeal of red raspberries to consumers largely arises from the berry's characteristic taste and aroma. Among the large number of volatile compounds identified, 4-(4-hydroxyphenyl)-2-butanone, commonly known as raspberry ketone (RK), is recognized as the primary compound responsible for the characteristic raspberry flavor [1–3]. In addition, RK is an FDA-designated generally recognized as safe (GRAS) additive, which has been widely used in the perfumery, cosmetics and food industry to impart raspberry aroma [4]. Due to its low abundance in nature, fruit-derived RK is among the most expensive natural flavor compounds with an estimated market value up to $20,000/kg [5]. Based on the structural similarity to other phenolic compounds (e.g., ephedrine, synephrine, and capsaicin and zingerone), RK also has been investigated as a putative weight loss supplement and appetite suppressant [6]. Rodent studies indicated that RK protected animals from high-fat diet-induced nonalcoholic steatohepatitis [7], prevented diet-induced obesity, and reduced the inclination towards high-fat diets [7,8]. *In vitro* studies also suggested that RK activates pathways that promotes fatty acid oxidation and reduces lipogenesis in adipocytes [9,10]. Therefore, having an effective methodology for measuring RK content in raspberries of all sources would better facilitate selection of raspberries that are more appealing to consumers and richer in bioactive components including RK.

The analysis of RK content in red raspberry sources has been predominated by GC-MS as reported in literature [1]. However, there is limited reliable study employing LC-MS methodologies to detect and measure content of RK in red raspberries and related products. In the study by Urska et al. in 2012, a targeted metabolomics method using LC-MS was established for analyzing up to 135 phenolics in fruit with RK included as one of the metabolites. This method, unfortunately, lacked specificity for RK and the limit of detection was not low enough to allow detection of RK in raspberries following direct sample preparation [11].

The aim of this study was to develop a rapid and sensitive method using ultra-high performance liquid chromatography (UHPLC) coupled with triple quadrupole mass spectrometry (QqQ-MS) for reliable quantification of RK in different sources of red raspberries to facilitate quality control, which could also be extended the application for RK pharmacokinetic study.

2. Experimental

2.1. Chemical reagents and raspberries

Reference standard of RK was purchased from Sigma–Aldrich (St. Louis, MO, USA). Methanol, acetic acid, and HPLC grade water and acetonitrile and formic acid were purchased from Fisher Scientific (Fair Lawn, NJ, USA). Fresh raspberry fruits at different stages of maturity were harvested from local New Jersey farms and stored at −20 °C prior to analysis. Fresh raspberries marketed as organic or non-organic products were purchased from local supermarkets, stored at 4 °C and then analyzed within two days of purchase. The harvest or purchase dates and location, and sample conditions are shown in Table 1.

2.2. Standard and sample preparation

For the standard preparation, approximately 10 mg of RK standard was accurately weighed and dissolved in 25 mL methanol as stock solution. This was further diluted with 70% methanol for use as the work solution. For sample preparation, frozen fresh fruits of raspberry were first ground with liquid nitrogen, and approximately 3 g was then subsampled, accurately weighed and extracted using 8 mL pure methanol. The mixture was vigorously vortexed for 1 min, sonicated for 5 min and then centrifuged at 3000 rpm for 10 min. The supernatant was transferred to a glass vial and the precipitate was extracted two more times with 8 mL methanol likewise. The supernatants were combined and brought to a final volume of 30 mL. The extract was then diluted 5-fold with 70% methanol and centrifuged at 13,000 rpm for 10 min prior to LC-MS injection. Three extracts were prepared for each raspberry sample. The final RK content was presented as μg/100 g fresh weight (FW).

2.3. Instrumentation

An Agilent 1100 series LC/MSD instrument (Agilent Technologies, Waldbronn, Germany) was used to facilitate determination of the precursor ion of RK. The HPLC was equipped with an auto-degasser, quaternary pump, column thermostat and a diode-array detector (DAD). Column Phenomenex Luna C18 (2), 150 × 4.60 mm, 5 μm (Torrance, CA) was used for compound separation. The LC-MS interface was electrospray ionization (ESI). Nitrogen was used as nebulizing gas and drying gas. The MS featured an ion trap analyzer and helium was used as the collision gas. Data was acquired using the Agilent ChemStation (ver A.08.03) and LC/MSD Trap Control (ver 5.1).

An Agilent 1290 Infinity II UHPLC coupled with 6470 triple quadrupole (QqQ) (Agilent Technologies, Waldbronn, Germany) was used for development of fully optimized method of quantification of RK. The UHPLC was equipped with a built-in auto-degasser, binary pump and column thermostat. The DAD was bypassed to reduce peak broadening. Waters Acquity BEH C18 column, 50 × 2.1 mm, 1.7 μm (Milford, MA) equipped with Waters Acquity UPLC BEH C8 VanGuard pre-column 5 × 2.1 mm, 1.7 μm (Milford, MA) was used for compound separation. The LC-MS interface was ESI with jet stream. Nitrogen was used as nebulizing gas, drying gas, sheath gas and collision gas. MassHunter Workstation LC/MS Data Acquisition (ver B.08.00) was used for data acquisition and MassHunter Workstation Optimizer (ver B.08.00) for MRM optimization.

2.4. Determination of precursor ion by ion trap MS

Agilent 1100 series ion trap MS was used for screening of the precursor ion. Specifically, for HPLC, mobile phase A was

Table 1 – Identification of the raspberry samples used in this study and their respective raspberry ketone concentration.

No.	Source/Brand	Purchase/Harvest location	Purchase/harvest time	Content (μg/kg FW)
1	Driscoll's, mature and red, USDA certified organic	Shoprite, Piscataway, NJ	October, 2017	293.5 ± 40.9
2	Driscoll's, mature and red	Target, Piscataway, NJ	October, 2017	82.0 ± 2.6
3	Driscoll's, mature and red, USDA certified organic	Target, Piscataway, NJ	October, 2017	93.9 ± 3.1
4	Driscoll's, mature and red	Stop & Shop, Piscataway, NJ	October, 2017	74.1 ± 14.5
5	Driscoll's, mature and red, USDA certified organic	Stop & Shop, Piscataway, NJ	October, 2017	296.0 ± 19.7
6	Driscoll's, mature and red, USDA certified organic, (trademark 1)	Trader Joe's, New Brunswick, NJ	October, 2017	40.2 ± 1.4
7	Driscoll's, mature and red, USDA certified organic, (trademark 2)	Trader Joe's, New Brunswick, NJ	October, 2017	9.9 ± 2.1
8	Farm berries, half mature, pink to red	Hacklebarney Farms Cider Mill, Chester, NJ	August, 2016	480.9 ± 24.0
9	Farm berries, mature, dark and deep red	Hacklebarney Farms Cider Mill, Chester, NJ	August, 2016	712.1 ± 67.0
10	Farm berries, half mature, pink to red	Rutgers University Cook Organic garden, New Brunswick, NJ	July, 2016	416.4 ± 60.0
11	Farm berries, mature, dark and deep red	Rutgers University Cook Organic garden, New Brunswick, NJ	July, 2016	622.0 ± 44.4

Notes: FW = fresh fruit weight.

water with 0.1% formic acid and mobile phase B was acetonitrile with 0.1% formic acid at a flow rate of 1 mL/min. The gradient started at 30% B at 0 min and increased to 60% B at 15 min. The injection volume was 20 μL and around 800 ng of RK was injected onto column. The column thermostat was set at 25 °C. The wavelength of DAD was set at 254 nm with the reference wavelength at 400 nm. About a third of the HPLC eluent was split into MS. For MS, the nebulizer was set at 40 psi, drying gas temperature at 350 °C with a flow rate of 12 L/min. The capillary voltage was +3500 V in positive scan and −3500 V in negative scan. Either positive or negative polarity was used in separate injections. The full scanning range of ion trap was from 50 to 500 *m*/z. Collision energy noted as compound stability was set at 80%, which generally allowed structurally similar small phenolic acids to retain integrity in the ion trap. Ion charge control (ICC) was set with a target of 40,000 with a maximum accumulation time of 300 ms.

2.5. *Determination of precursor ion by QqQ-MS*

Following the experiment using ion trap MS, Agilent 1290 UHPLC-6470 QqQ was used as the principal instrument in the successive studies. First, full scan mode was used to identify the precursor ion. For UHPLC, the mobile phase components were the same as in the ion trap experiment (section 2.4) with a flow rate of 0.4 mL/min. The injection volume was 5 μL and around 5.5 ng standard of RK was injected onto column. The column thermostat was set at 30 °C. With respect to QqQ-MS, the ESI was preliminary set as environment suitable for small phenolic acids with modification, i.e., nebulizer was set at 30 psi, drying gas temperature at 300 °C with a flow rate of 12.0 L/min, sheath gas temperature at 300 °C with a flow rate of 10.0 L/min, capillary voltage at +2500 V (positive scan) or −2500 V (negative scan), and nozzle voltage at +1000 V (positive scan) or −1000 V (negative scan) [12]. Either positive or negative polarity was used in separate injections. Three scan segments were included in one run, each segment having the same scan range from 50 to 200 *m*/z and scanning time of 500 ms but different fragmentor voltage (FV) (voltage applied to the exit end of the capillary) at 80, 110, and 140 V, respectively. The three FVs represented a reasonably wide range found to be suitable for structurally similar small phenolic acids [12]. The accuracy of the mass of the predominant ion, the prospective precursor, was further confirmed by full scan using narrower scanning range down to ±5 Da of the detected mass.

2.6. *Optimization of MRM transitions*

To facilitate MRM optimization, an isocratic gradient with 28% B was employed and the RK peak was eluted out within 1 min. Other parameters remained the same as those in the precursor confirmation study using QqQ (section 2.5) unless otherwise specialized. The most abundant RK fragment or cluster ions detected in section 2.5 was manually added to the MassHunter Optimizer as the prospective precursor, and then subjected to an optimization procedure composed of five consecutive injections under scanning modes of selected ion monitoring (SIM), SIM, product ion (PI) scan, MRM and then PI, respectively. The injection steps are shown in Table S1.

Around 5 ng of RK was injected onto column for SIM and MRM and 10 ng injected for PI scan to compensate for the low sensitivity of PI scan mode. The most abundant product ion was selected as the quantifier ion as the result of a successful optimization.

2.7. Optimization of ESI

The optimized MRM transitions so far acquired and relevant LC-MS conditions as aforementioned were applied for the optimization of ESI. Seven key parameters, i.e., drying gas temperature (X_1) and flow rate (X_2), nebulizer pressure (X_3), sheath gas temperature (X_4) and flow rate (X_5), capillary voltage (X_6) and nozzle voltage (X_7), were optimized by the design of experiment (DOE) approach using fractional factorial design. Two levels of each factor were tested by expanding the general setting to an empirically higher and lower end. As the instrumental sensitivity was dependent on signal response (peak area) and background noise, signal-to-noise ratio (S/N) was used as the DOE model response. Injections were made in triplicate for each trial and the averaged S/N was used as the response. The factorial design conditions are presented in Table S2.

2.8. Optimization of other parameters

For the UHPLC part, influences of mobile phase modifiers, i.e. formic acid and acetic acid at 0.1 or 0.2% on detection sensitivity were studied. For the QqQ MS part, the quadrupole resolution set at either "unit" or "wide" was compared for impact on detection sensitivity. The cell accelerator voltage was studied in a range of 4–8 V. The detector Delta EMV was fine-tuned ranging from 0 to 100 V.

2.9. Method validation

The method was validated in terms of linearity range, low limit of detection (LLOD), low limit of quantification (LLOQ), accuracy and intra-batch and inter-batch precision. The LLOD and LLOQ were defined as S/N ratio at 3 and 10, respectively. For accuracy validation, a known amount of RK standard was spiked in the quality control (QC) sample at 200%, 100% and 50% level of expected concentration, and accuracy was calculated as (detected concentration − endogenous concentration)/spiked concentration × 100%. Fresh raspberries manually harvested from the Rutgers University Cook College Campus Organic garden, New Brunswick, were used as the QC sample. Precision was calculated as the standard deviation of repeated injections in single sequence for intra-batch precision and separated sequences for inter-batch precision at three levels, i.e., LLOQ, middle point of linearity range (MP), and high limit of quantification (HLOQ).

2.10. Data analysis and statistics

Analysis of data acquired from Agilent 1100 LC-MS system was conducted by Agilent Data Analysis (ver 2.2). Analysis of data acquired from Agilent UHPLC-QqQ MS system was performed on MassHunter Workstation Qualitative Analysis (ver B.07.00) and Quantitative Analysis (ver B.07.01). Fractional factorial design was analyzed by Design Expert (ver 8.0.6).

3. Results and discussion

3.1. Method development and validation

3.1.1. Determination of precursor ions

Precursor ions that are protonated, deprotonated and adducted with cations such as sodium and ammonium are the most common precursors formed in the ESI compartment. However, selection of these most common ions as prospective precursors was found in the preliminary RK study failing to generate reliable product ions with strong MS responses. This suggested formation of cluster ions or severe in-source fragmentation in the ESI compartment. In view of the significantly lower sensitivity under full scan mode of triple quadrupole MS compared with ion-trap MS [13], screening for the possible cluster ion(s) and in-source fragment(s) was first conducted using ion-trap MS. As the ion trap MS featured analogous ESI configuration and parameters with those of QqQ MS, ionization behavior of RK observed in the ion trap MS study could provide valuable reference for the subsequent study using QqQ-MS.

The ion trap MS study conducted under positive polarity using low collision energy revealed low abundance of parent ions that were protonated ($[M+H]^+$, 165 *m/z*) or adducted with a sodium ion ($[M+Na]^+$, 187 *m/z*), while the predominant peak was detected at 107 *m/z* (Fig. 1). A separate analysis of RK under negative polarity did not generate any noticeable RK peak.

The major challenge in the following QqQ study was the low sensitivity of full scan and that RK peak was barely visible in total ion chromatogram (TIC), as shown in Fig. 2 inset. Considering that the injected concentration (5.5 ng injected

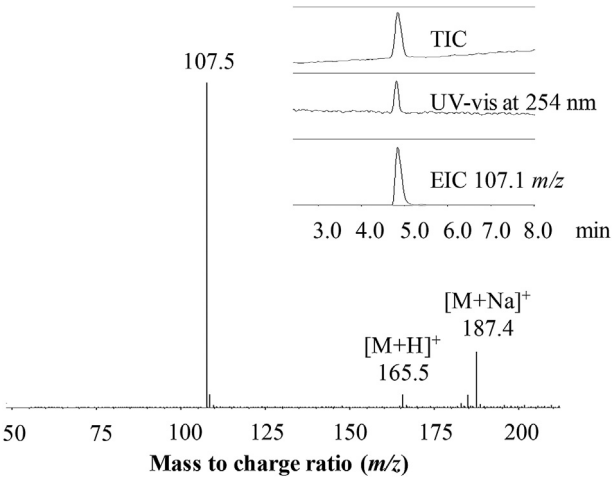

Fig. 1 – Mass spectrum of raspberry ketone as acquired by ion trap MS. Inset was the corresponding chromatograms of total ion (TIC), UV–vis at 254 nm and that of extracted ion (EIC) of the major fragment at 107. 1 *m/z* with 800 ng raspberry ketone injected on column.

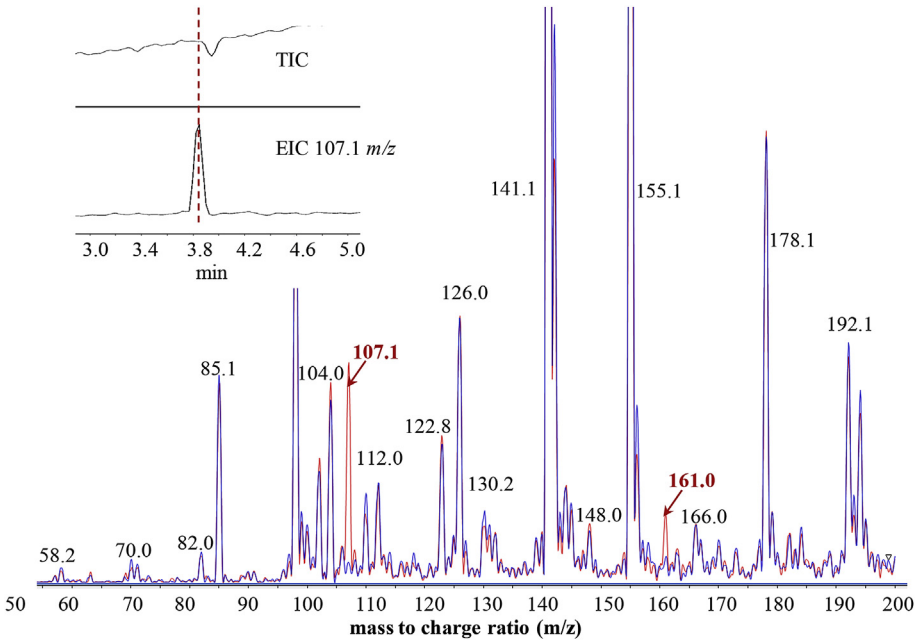

Fig. 2 – Overlaid mass spectra of raspberry ketone (RK) and background acquired by QqQ MS. Mass spectrum of RK (red) was acquired at 3.8 min and background (blue) at 4.6 min. Fragmentor voltage was preliminary set at 110 V. Inset in the upper left was the corresponding chromatograms with 5.5 ng of RK injected on column. Notice the near invisibility of RK peak in total ion chromatogram (TIC). RK peak was rendered visible by extracted ion chromatogram (EIC). 161.0 *m/z* was a random ion from the background.

onto column) was already on the high end, injection of higher concentration to improve peak visibility was avoided to prevent contamination. With reference to the aforementioned ion trap study, the positively charged ion at 107 *m/z* was tentatively extracted and this successfully led to identification of RK peak at 3.8 min. Careful comparison of the mass spectra of RK with that of the background confirmed the actual MS response of the ion at 107 *m/z* and lack of detectable protonated and adducted parent ions (Fig. 2). This explained the unsuccessful detection of RK in the preliminary study inappropriately selecting protonated or adducted parent ions as the precursor ions. In addition, negative polarity did not generate significant RK peak on QqQ MS either. Thus, the positive 107 *m/z* ion formed as the result of in-source fragmentation was selected as the precursor ion for the subsequent MRM study using QqQ MS.

3.1.2. *Optimization of MRM transitions*

Optimization of MRM transitions can be most conveniently achieved via injection mode instead of the conventional infusion method. Under this injection mode, a connection union can be used in replacement of an analytical column thus without compound separation, so that each injection could be finished within 10 s. Usage of connection union in the case of RK, however, seemed to result in less accurate "locking" of the characteristic 107 *m/z* ions during the fragmentor voltage (FV)-optimization injections and led to questionable optimized data. This was realized by comparison of the inaccurately optimized MRM transitions with the corresponding transitions under SIM mode using the same precursor. The inefficiency of optimization was manifested by insignificant improvement or even reduction in S/N acquired under MRM versus SIM mode, as shown in Fig. S1. This optimization inadequacy might be a result of interference from isobaric impurities in the injected solvent, which simultaneously entered ESI compartment with RK without column separation.

Thus, an analytical column was used to replace the connection union so as to chromatographically separate RK from possible solvent impurities and to facilitate targeting at the 107 *m/z* ions. Under isocratic elution with 28% B, RK could be timely eluted out at around 1 min with adequate separation from the background impurities, with one optimization cycle (five injections) finished within minutes. The optimization procedure using column was shown in Fig. 3 and the corresponding key parameters were listed in Table S1. This led to improved optimization efficiency as shown in Fig. S2. The eventual optimization result was FV at 130 V and quantifier ion at 77.1 *m/z* under CE 25 eV.

3.1.3. *Optimization of ESI*

Unlike most compounds that get ionized remaining intact in the ESI, the intense in-source fragmentation as well as the moderate volatility of RK required the ESI settings to be particularly optimized to achieve the optimal sensitivity. Fractional factorial design was applied to optimize and evaluate the significance of different ESI setting variables and interactions involved, and to reduce trial numbers without losing essential information [14]. The conditions used in the fractional factorial design were included in Table S2.

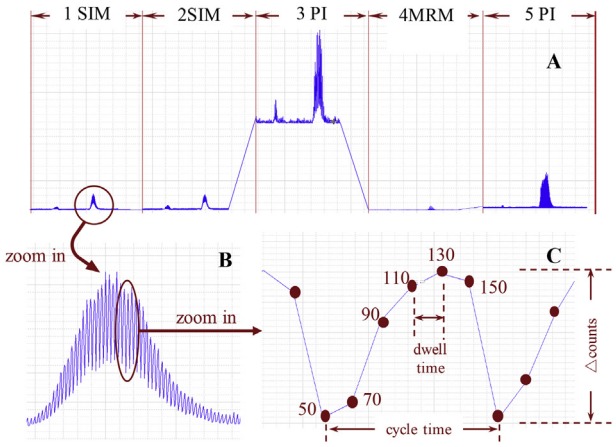

Fig. 3 – Real time optimization chromatograms of raspberry ketone (RK). (A), chromatographic overview of five consecutive injections and scanning mode; (B), zoomed-in peak of RK in the first SIM injection; (C) zoomed-in data points (red dots) showing varied signal counts under different fragmentor voltage (numbers). x-axis was time and y -axis signal counts and not shown for clarity. The corresponding settings were shown in Table S1. Notice the 'sawtooth-like' peak curve and "filling" effect under the peak curve due to △counts, which indicated differences in sensitivity of signal counts according to the given varying parameter. Also notice the high counts and low S/N in product ion (PI) scan, compared with the low counts and high S/N in MRM.

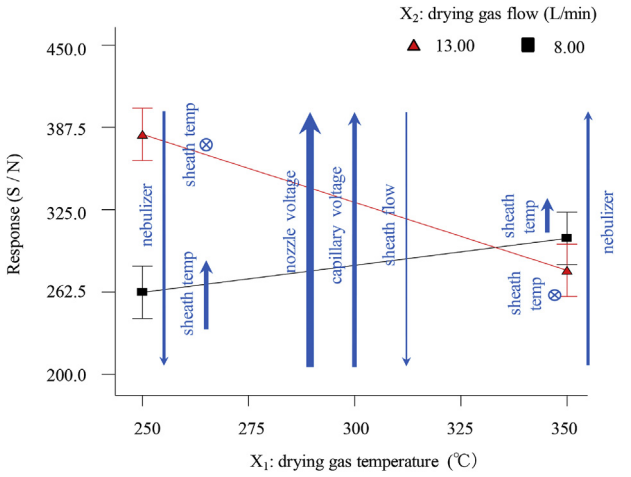

Fig. 4 – Impact of ESI settings to signal/noise ratio based on fractional factorial design model. Upward arrows indicate increase in S/N when the corresponding setting increases, and downward arrows indicate increase in S/N when the setting is tuned down. Circled cross indicates negligible influence. Arrows at the plot center indicate direction of vertical gliding of the entire plot when the given variables are changed. Arrows at the two sides indicate independent shifting of separated data points. Temp is short for temperature.

The function using factor codes was established as $Y = -15.56X_1 + 23.94X_2 - 2.69X_3 + 12.44X_4 - 13.69X_5 + 17.31X_6 + 42.81X_7 - 36.06X_1X_2 + 19.56X_1X_3 - 15.81X_2X_4 + 306.69$, $R^2 = 0.9722$, and adjusted $R^2 = 0.9166$. The influence and interactions among the seven ESI parameters are schematically depicted in Fig. 4. Among the gas-related parameters, S/N was most effectively modulated by changing the temperature and flow rate of drying gas and meantime also fine-tuned by others. When the drying gas flow rate was low, simultaneous elevation in drying and sheath gas temperature and nebulizer pressure significantly increased S/N, presumably by increasing the evaporation of solvent in and thus RK desorption from the electrosprayed aerosol. At higher drying gas flow rate, in contrast, optimal S/N could be achieved by reduction in both drying gas temperature and nebulizer pressure. Change in sheath gas temperature had little impact on S/N when the drying gas flow was high. Sheath gas flow was found to be the least important factor with a slight negative impact on S/N. The two voltage settings, nozzle and capillary voltage both had noticeably positive impact on S/N, especially the former being the single most influential in all seven parameters. Higher nozzle voltage beyond the experimented upper bound only generated minor improvement in S/N. Considering all factors collectively, the optimal setting for all seven parameters were determined as drying gas at 250 °C with a flow rate at 13 L/min, nebulizer at 25 psi, sheath gas at 300 °C with a flow rate at 8 L/min, capillary voltage of 3000 V and nozzle voltage of 1500 V.

3.1.4. *Optimization of other settings*

The two most commonly used mobile phase modifiers, formic acid and acetic acid, were found to have important impact on instrumental performance. Acetic acid at 0.1% gave the best S/N, and a higher concentration at 0.2% led to marginal reduction in S/N. Addition of formic acid resulted in lower S/N than acetic acid at the same concentrations. Particularly, formic acid at 0.2% led to nearly two times reduction in S/N than 0.2% acetic acid. Mobile phase without modification with formic or acetic acid resulted in high background and low signal response and thus the lowest S/N. Therefore, 0.1% acetic acid was selected as the optimal mobile phase modifier.

The quadrupole resolution setting defines broadness of the ionic filtration window. Quadrupole resolution set in "unit", filtration window of 0.7 Da wide, was found to give higher S/N than resolution in "wide", which had a filtration window of 1.2 Da wide, by reduction of background noise. Cell accelerator voltage (CAV) was the voltage gradient applied to the collision cell to increase drifting velocity of ions traversing the collision cell and hence to prevent stalling of ions in collision cell and cross-talk between MRMs, the latter being a phenomenon of one ongoing MRM transition getting "contaminated" by product ions produced by the last transition. The range CAV adjusted was from 4 to 8 V, and comparable S/N ratios were obtained. CAV was then set to 5 V. Delta EMV was the extra voltage applied to the detector and adjusted as the last resort for fine tune of sensitivity. S/N increased by around 20% with the elevation of Delta EMV from 10 to 20 V, reached its

Table 2 – Validation of method for quantification of raspberry ketone.

LLOD (ng/ml)	LLOQ (ng/ml)	Linear range (ng/ml)	Calibration curve	R^2
0.97[a]	1.95[a]	1.95~998.90	Y = 33.380 X + 29.634	0.9951[c]

Accuracy (%)[b]			Intra-batch precision (%)			Inter-batch precision (%)		
50% level	100% level	200% level	LLOQ	MP	HLOQ	LLOQ	MP	HLOQ
102.7	101.7	116.9	13.8	1.6	2.8	17.6	8.6	8.3

Quant, quantifier ion; LLOD, low limit of detection; LLOQ, low limit of quantification; MP, middle point of linearity range; HLOQ, high limit of quantification. [a]LLOD and LLOQ were acquired with 3 μL injection volume, corresponding to 2.91 pg and 5.85 pg injected on column, respectively. [b]The percentage levels for accuracy refers to the percentage of expected RK concentration in the QC sample. [c]R^2 was calculated with 1/x weight.

maximum at around 30 ± 10 V, and then decreased slightly and plateaued at higher Delta EMV. Accordingly, the optimal Delta EMV value was set at 30 V.

3.1.5. *Optimized method and validation*

The optimized method was summarized as below. For the UHPLC part, water with 0.1% acetic acid was used as mobile phase A, and acetonitrile with 0.1% acetic acid was used as mobile phase B. The flow rate was 0.4 mL/min. The gradient started at 28% B, held for 1.2 min, then increased to 100% B at 1.3 min and held for 1 min before returning to initial conditions. Eluent between 0 and 0.8 min and after 1.2 min was directed into waste. The column was equilibrated with 28% B for 1.5 min between injections. The column was thermostatted at 30 °C. The injection volume was 3 μL. For the QqQ part, the ESI featured a setting of drying gas at 250 °C with a flow rate of 13 L/min, nebulizer at 25 psi, sheath gas at 300 °C with a flow rate of 8 L/min, capillary voltage of 3000 V and nozzle voltage of 1500 V. The precursor ion was 107 *m/z* with FV at 130 V, and product ions were 77.1 *m/z* with CE of 25 eV as the quantifier ion. Dwell time was 30 ms. The quadruple resolution was "unit". CAV was at 5. Delta EMV value was +30 V. Representative MRM chromatograms of standard solution of RK are shown in Fig. S3.

The validation result of the method as summarized in Table 2 shows excellent accuracy and precision for quantification. The LLOQ was 2 ng/mL or 6 pg injected on column and was low enough to allow for detection of trace level of RK in fresh raspberries following routine analysis. The linearity range had three orders of magnitude, allowing for detection of samples with large dynamic range of content of RK. Accuracies of all QC levels were less than 20% off the expected value. Intra-batch precision was excellent for MP and HLOQ, with all less than 3% deviation, and precision at LLOQ was below 15%. Inter-batch precision as expected showed higher deviation but all below 18% for the three levels validated.

3.2. *RK fragmentation behavior*

The fragmentation pathway of RK could be rationalized as shown in Fig. S4-A. The intense in-source fragmentation of RK could be favored by formation of highly stable fragments with extended conjugation. A possible mechanism started with protonation on the carbonyl site due to its high electronegativity, which triggered electron delocalization for structure rearrangement. This resulted in the cleavage of β bond, a neutral loss of propen-2-ol, and migration of the positive charge to the fragmental ion of 107 *m/z* which had a formula of $C_7H_7O^+$ suggested by high-resolution MS (see Fig. S4-B) with a proposed conjugated quinone-like structure [15,16]. The precursor ion 107 *m/z* further experienced net loss of CH_2O in the collision cell to form ion 77 *m/z* with formula of $C_6H_5^+$ (see Fig. S4-C) [15]. The positive charge in the product ion was stabilized by the conjugated double bonds. The identities of major fragments were further confirmed by HR-MS.

3.3. *Quantification of RK in raspberries*

Most published studies related to RK analysis can be dated back to early 1990s, with a broad concentration range reported in raspberries. RK levels were commonly reported in the range of 10–700 μg/kg fresh weight (FW) [17,18], yet one was reported to be up to 4000 μg/kg FW [2]. In this study, fresh raspberries labeled as certified organic or non-organic products were purchased from four different local supermarkets, and cultivated berries at different stages of maturation were harvested from two local farms. RK was then extracted and quantified. The contents were also found to be divergent, ranging from 10 to 600 μg RK/kg FW, which was within the typical range as previously reported [17,18]. The RK content levels detected are summarized in Table 1. Representative chromatograms of RK in the raspberry extract are shown in Fig. S3. There was a significant difference in RK concentrations among raspberries of the same brand purchased from different supermarkets. While the objective was not to compare total RK relative to what is 'best' but only to ensure the sensitivity of this new method could differentiate the content in different berry sources, the levels of RK did not bear significantly relationship with the screened "organic" or "non-organic" products. There is a significant recognized impact by production and postharvest handling systems, by genetics (e.g. varieties) and seasonal impacts that would impact fruit quality. A strikingly higher level of RK was found in the farm berries than those commercially marketed. As hypothesized, the mature berries contained much higher RK than those only partially mature or artificially ripened.

4. Conclusion

A UHPLC-QqQ/MS method for rapid and sensitive quantification of RK was successfully developed and validated. In particular, full scan experiment using both ion-trap MS and QqQ MS revealed severe in-source fragmentation of RK.

Potential mechanism of fragmentation in the ESI and collision cell was proposed for the first time. In view of the unusual in-source fragmentation as well as high volatility of RK, settings for ESI were specially optimized using fractional factorial design, which effectively enhanced the sensitivity. Further, the findings from this study indicate that RK concentration in commercial and farm berries can be vastly different. This discrepancy could be related to selection process adopted by commercial manufacturers before bringing berries to market. In this regard, organic labeling has little correlation with RK content. A difference in the maturity stage, however, is more likely to influence RK content. Late-stage maturity raspberries were found to have higher RK content, which suggests that RK accumulates with increasing maturity, and this agrees with earlier reports [1]. One limitation of the present study is that there is no sensory evaluation of the red raspberry for taste or aroma. Future work needs to examine the accumulation pattern over a wider degree of fruit maturation. In addition, there is a need to determine influencing factors of RK contents, including light and oxidation, source-sink relationships and other environmental conditions.

Acknowledgement

This research was supported by the NIH project (R01AT008933), "*Effects of raspberry ketone on body weight and metabolic outcomes in obesity*", awarded to Bello and Wu. Additional funds were provided by the New Jersey Agriculture Experiment Station, Hatch Project 12131.

Appendix A. Supplementary data

Supplementary data related to this article can be found at https://doi.org/10.1016/j.jfda.2018.07.005.

REFERENCES

[1] Aprea E, Biasioli F, Gasperi F. Volatile compounds of raspberry fruit: from analytical methods to biological role and sensory impact. Molecules 2015;20:2445–74.
[2] Larsen M, Poll L, Callesen O, Lewis M. Relations between the content of aroma compounds and the sensory evaluation of 10 raspberry varieties (*Rubus idaeus* L). Acta Agric Scand 1991;41:447–54.
[3] Honkanen E, Pyysalo T, Hirvi T. The aroma of Finnish wild raspberries, *Rubus idaeus*, L. Zeitschrift für Lebensmitteluntersuchung und-Forschung A 1980;171:180–2.
[4] Bredsdorff L, Wedebye EB, Nikolov NG, Hallas-Moller T, Pilegaard K. Raspberry ketone in food supplements–High intake, few toxicity data–A cause for safety concern? Regul Toxicol Pharmacol 2015;73:196–200.
[5] Beekwilder J, van der Meer IM, Sibbesen O, Broekgaarden M, Qvist I, Mikkelsen JD, et al. Microbial production of natural raspberry ketone. Biotechnol J 2007;2:1270–9.
[6] Wang L, Meng X, Zhang F. Raspberry ketone protects rats fed high-fat diets against nonalcoholic steatohepatitis. J Med Food 2012;15:495–503.
[7] Morimoto C, Satoh Y, Hara M, Inoue S, Tsujita T, Okuda H. Anti-obese action of raspberry ketone. Life Sci 2005;77:194–204.
[8] Cotten BM, Diamond SA, Banh T, Hsiao Y-H, Cole RM, Li J, et al. Raspberry ketone fails to reduce adiposity beyond decreasing food intake in C57BL/6 mice fed a high-fat diet. Food Funct 2017;8:1512–8.
[9] Park KS. Raspberry ketone, a naturally occurring phenolic compound, inhibits adipogenic and lipogenic gene expression in 3T3-L1 adipocytes. Pharm Biol 2015;53:870–5.
[10] Park KS. Raspberry ketone increases both lipolysis and fatty acid oxidation in 3T3-L1 adipocytes. Planta Med 2010;76:1654–8.
[11] Vrhovsek U, Masuero D, Gasperotti M, Franceschi P, Caputi L, Viola R, et al. A versatile targeted metabolomics method for the rapid quantification of multiple classes of phenolics in fruits and beverages. J Agric Food Chem 2012;60:8831–40.
[12] Zhao D, Yuan Bo, Carry E, Pasinetti GM, Ho L, Faith J, et al. Development and validation of an ultra-high performance liquid chromatography/triple quadrupole tandem mass spectrometry method for analyzing microbial-derived grape polyphenol metabolites. Manuscript in revision. J Chromatogr B 2018.
[13] Johnson AR, Carlson EE. Collision-induced dissociation mass spectrometry: a powerful tool for natural product structure elucidation. Anal Chem 2015;87:10668–78.
[14] Martendal E, Budziak D, Carasek E. Application of fractional factorial experimental and Box-Behnken designs for optimization of single-drop microextraction of 2,4,6-trichloroanisole and 2,4,6-tribromoanisole from wine samples. J Chromatogr A 2007;1148:131–6.
[15] ChemCalc: a building block for tomorrow's chemical infrastructure. Patiny Luc Borel Alain J Chem Inf Model 2013. https://doi.org/10.1021/ci300563h.
[16] Fredenhagen A, Derrien C, Gassmann E. An MS/MS library on an ion-trap instrument for efficient dereplication of natural products. Different fragmentation patterns for $[M + H]^+$ and $[M + Na]^+$ ions. J Nat Prod 2005;68:385–91.
[17] Borejsza-Wysocki W, Goers SK, McArdle RN, Hrazdina G. (p-Hydroxyphenyl) butan-2-one levels in raspberries determined by chromatographic and organoleptic methods. J Agric Food Chem 1992;40:1176–7.
[18] Maquin F, Meili M, Chaveron H. Determination of 4-(p-hydroxyphenyl)-2-butanone by mass fragmentometry. Ann Falsif Expert Chim Toxicol 1981;74:511–21.